

Adaptive Polynomial Chaos for Gas Turbine Compression Systems Performance Analysis

Tiziano Ghisu,* Geoffrey T. Parks,† Jerome P. Jarrett,‡ and P. John Clarkson§
University of Cambridge, Cambridge, England CB2 1PZ, United Kingdom

DOI: 10.2514/1.J050012

The design of a gas turbine, or one of its constituent modules, is generally approached with some specific operating condition in mind (its design point). Unfortunately, engine components seldom exactly meet their specifications and do not operate at just one condition, but over a range of power settings. This simplification can then lead to a product that exhibits performance worse than nominal in real-world conditions. The integration of some consideration of robustness as an active part of the design process can allow products less sensitive to the presence of the noise factors commonly found in real-world environments to be obtained. To become routinely used as a design tool, minimization of the time required for robustness analysis is paramount. In this study, a nonintrusive polynomial chaos formulation is used to evaluate the variability in the performance of a generic modular-core compression system for a three-spool modern gas turbine engine subject to uncertain operating conditions with a defined probability density function. The standard orthogonal polynomials from the Askey scheme are replaced by a set of orthonormal polynomials calculated relative to the specific probability density function, improving the convergence of the method.

Nomenclature

A_m, B_m, C_m	= coefficients of the recurrence relation for generic orthogonal polynomials	δ_{ij}	= Kronecker delta
$b_{i,j}$	= adaptive orthogonal polynomial coefficient	η	= isentropic efficiency
$b_{i,j}^*$	= adaptive orthonormal polynomial coefficient	η_{tot}	= total system isentropic efficiency
c_1, c_2	= coefficients of the recurrence relation for monic orthogonal polynomials	μ	= mean value
f	= objective function	ξ_i	= support random variable
H_v	= fuel lower calorific value	ξ	= vector of support random variables
I_i	= generic Wiener–Askey polynomial	Π_i	= multidimensional adaptive orthonormal polynomial
k	= generic input variable	σ^2	= variance
m	= number of simulations	τ_i	= input uncertainty
\bar{m}	= pseudo-non-dimensional mass flow	Φ_i	= Wiener–Askey chaos
\dot{m}	= mass flow	ω	= duct total pressure loss
N	= number of random dimensions		
N_0	= quadrature order		
N_t	= number of collocation points		
P	= total pressure		
PR	= pressure ratio		
P_i^*	= adaptive orthonormal polynomial		
P_i	= adaptive orthogonal polynomial		
SM	= surge margin		
s^3	= skew		
T	= total temperature		
W	= weighting function		
\dot{W}	= power		
w	= weight factor		
x	= design vector		
Y	= random process		
γ_i	= random-process expansion coefficient		
$\alpha_m, \beta_m, \gamma_m$	= coefficients of the recurrence relation for orthonormal polynomials		
γ	= ratio of specific heats		

Subscripts

HPC	= high-pressure compressor
IPC	= intermediate-pressure compressor
0	= total (stagnation) conditions

Introduction

ENGINEERING design commonly assumes nominal values for uncertain parameters to simplify the design process. Unfortunately, this simplification can lead to a product that exhibits performance worse than nominal in real-world conditions. This problem is exacerbated in the presence of heavily optimized designs, which tend to lie in extreme regions of the design space [1]. In real-world applications, it is important to not only achieve good performance, but also to be able to maintain it over a range of operating conditions and during the whole course of the life of the product. Some consideration of the impact of offdesign conditions on performance should therefore be embedded in the design process to avoid bigger problems during the later development or testing phases. Two different (but equivalent) illustrations of the concept of robust design are given in Fig. 1.

The causes of performance variability are usually defined as *noise factors*. A robust design is a design that is less sensitive to the presence of noise factors, which are categorized by Phadke [2] into three groups: *external* sources of performance variation that are independent of the product itself, *unit-to-unit* variation due to manufacturing variability (or manufacturing tolerances), and variation due to the *deterioration* in product performance with time and wear.

Modern engineering design relies heavily on a number of evermore-sophisticated computational models. These can represent an

Received 18 June 2009; revision received 27 December 2009; accepted for publication 6 January 2010. Copyright © 2009 by the authors. All rights reserved. Copies of this paper may be made for personal or internal use, on condition that the copier pay the \$10.00 per-copy fee to the Copyright Clearance Center, Inc., 222 Rosewood Drive, Danvers, MA 01923; include the code 0001-1452/10 and \$10.00 in correspondence with the CCC.

*Research Associate, Department of Engineering, Trumpington Street. Member AIAA.

†Senior Lecturer, Department of Engineering, Trumpington Street.

‡University Lecturer, Department of Engineering, Trumpington Street. Member AIAA.

§Professor, Department of Engineering, Trumpington Street.

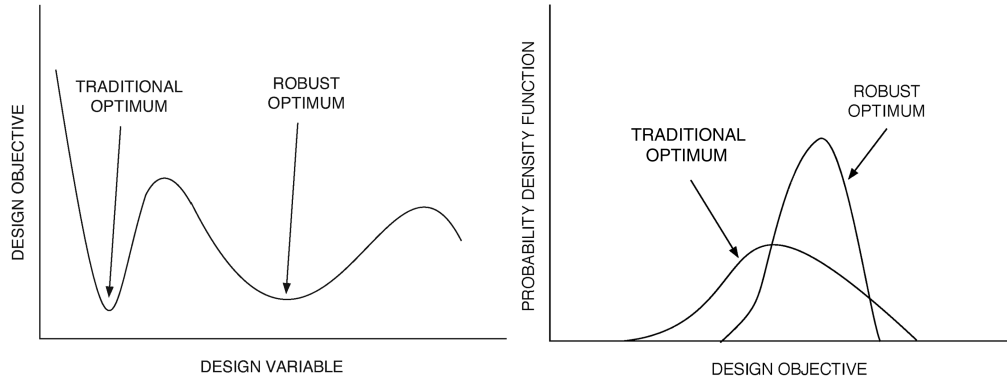


Fig. 1 Two different (but equivalent) illustrations of the concept of robust design.

additional source of uncertainty in the product's performance. A more realistic classification of uncertainty sources is given by Oberkampf and Trucano [3], who distinguish between *aleatory* and *epistemic* uncertainty: the former is associated with the physical system under consideration and its operating environment (already identified by Phadke [2]), and the latter arises from lack of knowledge in the modeling process and can be made negligible if sufficient data are available [1]. Walters and Huyse [4] concentrate on the role of uncertainty in computational fluid dynamics (CFD), further subdividing epistemic uncertainty into discretization and model uncertainty; discretization errors can be driven to zero (or to very low levels) with sufficient computational resources, whereas model uncertainty can be only estimated by comparing experimental and computational results.

Robust optimization can be considered as the methodology for finding the set of control factors (or design variables) that minimize the sensitivity of the product to the noise factors. Putko et al. [5] subdivide the whole process into three steps:

- 1) *Uncertainty quantification* is the determination of noise factors and their distribution.
- 2) *Uncertainty propagation* is the determination of the effect of the noise factors on the performance of the product.
- 3) *Robust optimization* itself is identification and selection of the best solution.

Walters and Huyse [4] give a comprehensive overview of the principal methods available for uncertainty analysis (focusing on fluid mechanics applications), separating deterministic methods (such as interval analysis and sensitivity derivatives), which are based on a number of deterministic evaluations and are relatively inexpensive, from probabilistic ones [Monte Carlo simulations (MCS), moments methods, and polynomial chaos] that attempt to approximate the probability distribution of the objective function, but are computationally more expensive and require a more detailed estimation of the probability distribution of the noise factors.

The essential strategy of the *interval analysis* approach is to evaluate the performance of the system for a number of combinations of the noise factors to produce an estimation of the maximal error bounds for the nominal performance (or, equivalently, a worst-case-scenario evaluation). A similar estimation can be performed with *sensitivity derivatives* and a first-order Taylor series approximation of the objective function:

$$\Delta f = \sqrt{\sum_{i=1}^N \left[\frac{\partial f}{\partial \xi_i} \Delta \xi_i \right]^2} \quad (1)$$

where N is the number of uncertain parameters and $\Delta \xi_i$ are their uncertainty bounds.

Given an accurate estimation of the noise factors' probability distributions, Monte Carlo simulations represent the only method that allows an exact estimation of the probability distribution of the objective function (and then of its moments). The major limitation is the number of simulations needed to achieve an accurate estimation (the convergence rate of MCS is $\mathcal{O}(1/\sqrt{m})$, which means that the

number of samples has to be increased by a factor of 100 to improve the accuracy by one decimal place [1]); this is why, for real-world applications, this technique is generally used in association with some sort of response surface.

Moment methods are based on an approximation of the objective function f through a Taylor series expansion about its nominal value $\bar{f} = f(\bar{\xi})$. If only one uncertain parameter is considered, a second-order expansion of the objective function reads

$$f(\xi) = f(\bar{\xi}) + \frac{\partial f}{\partial \xi}(\Delta \xi) + \frac{1}{2} \frac{\partial^2 f}{\partial \xi^2}(\Delta \xi)^2 + \mathcal{O}(\Delta \xi^3) \quad (2)$$

First-order first-moment, first-order second-moment, second-order first-moment (SOFM), and second-order second-moment (SOSM) approaches take their names from the order of the expansion considered and of the moment analyzed. SOFM and SOSM can be calculated as follows:

$$\begin{aligned} \mu_f &= \int_{-\infty}^{\infty} f(\xi) p(\xi) d\xi = \int_{-\infty}^{\infty} \left[f(\bar{\xi}) + \frac{\partial f}{\partial \xi}(\Delta \xi) \right. \\ &\quad \left. + \frac{1}{2} \frac{\partial^2 f}{\partial \xi^2}(\Delta \xi)^2 \right] p(\xi) d\xi = f(\bar{\xi}) + \frac{\sigma^2(\xi)}{2} \frac{\partial^2 f}{\partial \xi^2} \Big|_{\bar{\xi}} \end{aligned} \quad (3)$$

$$\begin{aligned} \sigma_f^2 &= \int_{-\infty}^{\infty} [f(\xi) - f(\bar{\xi})]^2 p(\xi) d\xi = \int_{-\infty}^{\infty} \left[\frac{\partial f}{\partial \xi}(\Delta \xi) \right. \\ &\quad \left. + \frac{1}{2} \frac{\partial^2 f}{\partial \xi^2}(\Delta \xi)^2 \right]^2 p(\xi) d\xi = \left(\frac{\partial f}{\partial \xi} \Big|_{\bar{\xi}} \right)^2 \sigma^2(\xi) + \frac{3}{4} \left(\frac{\partial^2 f}{\partial \xi^2} \right)^2 \sigma^4(\xi) \end{aligned} \quad (4)$$

where $p(\xi)$ represents the noise factor's probability density function (PDF).

The above approximations are exact only when the noise factors are Gaussian-distributed and the objective function is well represented by a second-order Taylor series. The more the noise factors and the objective function(s) depart from these assumptions, the less reliable these estimates are.

In recent years, polynomial chaos (PC) has received much attention, as it offers an exact means of propagating uncertainties through a system, providing high-order information (similar to MCS) at a much reduced cost [6].

The roots of PC are to be found in the homogeneous chaos expansion first proposed by Wiener [7], who employs Hermite polynomials in terms of Gaussian random variables to express stochastic processes with finite variance. Cameron and Martin [8] demonstrate that "any Fourier-Hermite series of any functional $F(x)$ of $L_2(C)$ converges in the $L_2(C)$ sense to $F(x)$ " (i.e., any variable with finite variance, or second-order, can be represented exactly through the above-mentioned homogeneous chaos expansion). The natural application is modeling uncertainty propagation in physical applications; stochastic differential equations can be solved based on a truncated PC representation, employing Galerkin projections onto a finite subspace spanned by these polynomials as a way of simplifying the equations themselves [9].

Although the Cameron–Martin theorem ensures the convergence of the Hermite expansion for any second-order random process, the convergence rate is optimal (exponential) only in the case of Gaussian-distributed input uncertainties [10]. Xiu and Karniadakis [11] extend the original Wiener chaos by replacing the orthogonal Hermite polynomials with any set of orthogonal polynomials from the Askey scheme of hypergeometric orthogonal polynomials (see Table 1), the generalized PC (gPC), and numerically proving the exponential convergence of the so-called Wiener–Askey PC expansion for each set of orthogonal polynomials and its corresponding stochastic process. Wan and Karniadakis [12] develop a multi-element gPC approach to address the problem of high-order chaos required for accurate long-term integrations encountered by the standard gPC approach. The method is based on a decomposition of the stochastic input's random space into smaller elements and on a local application of the gPC approach, possible through the definition of a conditional probability density function and of a set of numerically generated orthogonal polynomials. This approach is particularly beneficial in the presence of long-term integration problems, large perturbations, and stochastic discontinuities. The method is demonstrated on a number of standard PDFs, but could be used also for treating arbitrary stochastic inputs.

One of the most widely known PC implementations is due to Ghanem and Spanos [9], who used Hermite polynomials in terms of Gaussian-distributed random processes to model the propagation of input uncertainties in solid mechanics and structural applications [13,14]. The first fluid mechanics implementations, both for incompressible laminar flows, are due to Le Maître et al. (solution of a natural convection problem in a two-dimensional square cavity with uncertain boundary conditions [15] and of a two-dimensional diffusion problem with uncertain diffusion coefficient and boundary conditions [16]) and to Xiu et al. (pressure-driven channel flow with uncertain boundary conditions, flow past a circular cylinder with uncertain inlet velocity [17], and flow-structure interaction in the vortex-induced vibration of an elastically mounted circular cylinder with uncertain parameters [6]). Their results present the same accuracy as from MCS with a three-order-of-magnitude reduction in the computational time. Since then, PC has been applied successfully to the evaluation of the effect of geometric uncertainties in diffusion [18] or convection–diffusion problems [19] for compressible laminar two-dimensional flows [19] and one-dimensional compressible turbulent flows (Mathelin et al. [20] study the effect of uncertainties in the geometry in the boundary conditions and in the coefficients of the k - ϵ turbulence model used to simulate the flow in a supersonic divergent nozzle). However, its implementation for more complex applications still remains a problem, because of the nonlinear nature of the Navier–Stokes equations that requires, for example, a 12-dimensional summation in the turbulent kinetic energy equation, even for a simple (in the deterministic sense) one-dimensional nozzle flow [20].

Debusschere et al. [21] highlight some of the main limitations of the PC approach: intrusiveness, large truncation errors in high-order polynomials, and difficult representation of nonpolynomial functions. Le Maître et al. [15] develop a nonintrusive alternative, based on the observation that the coefficients of the different modes can be obtained by projecting deterministic computations onto the

PC basis, preserving the same accuracy as the standard formulation with a still much reduced cost in comparison with the Monte Carlo approach, avoiding the modification of complex or not easily accessible computational codes required by the intrusive approach. Other examples of nonintrusive PC formulations are given by Mathelin and Hussaini [22], who use a collocation method in the analysis of the flow in a one-dimensional supersonic nozzle with uncertain boundary conditions; by Loeven et al. [23] in the solution of a linear piston problem (a one-dimensional fluid bounded by a mass attached to a spring), with uncertain spring stiffness and of the flow around a NACA0012 airfoil with uncertain flow Mach number; and by Hosder et al. [24] in the simulation of the inviscid flow around a three-dimensional wing with uncertain Mach number and angle of attack.

Model

This study aims to evaluate the variability in the performance of a generic modular-core compression system from a three-spool modern aeroengine [sketched in Fig. 2 and composed of an intermediate-pressure compressor (IPC), an S-shaped duct, and a high-pressure compressor (HPC)] subject to variability in the operating point, given in terms of its probability density function.

A proprietary code for mean line performance prediction is used for compressor analysis. Given geometry and operating point, the code estimates the performance in terms of efficiency and operating margin, both at design-point and offdesign conditions. At the design point, blade angles are calculated based on the prescribed design-point pressure-ratio distribution and air angles by application of the continuity equation coupled with a number of empirical correlations for boundary-layer development, blade incidence, and deviation. At offdesign conditions the prescribed mass flow and rotational speed are used to calculate boundary-layer development, incidence, and deviation and then losses and efficiencies. A prediction for the surge margin is also made based on a number of different correlations. The percentage surge margin is calculated as a function of the actual total pressure ratio and the pressure ratio at surge:

$$SM = \frac{PR_{\text{surge}} - PR}{PR} 100$$

The finite volume axisymmetric CFD solver developed by Ghisu [25] has been used to evaluate the performance of the S-shaped ducts and further to examine the effects of intermodule interface constraints on system performance [26].

The system isentropic efficiency can be calculated with the assumption of adiabatic flow, given the separate modules' performances:

$$\eta_{\text{tot}} = \frac{(PR_{\text{IPC}} PR_{\text{HPC}})^{\frac{\gamma-1}{\gamma}} (1 - \omega)^{\frac{\gamma-1}{\gamma}} - 1}{\left(\frac{PR_{\text{IPC}}^{\frac{\gamma-1}{\gamma}} - 1}{\eta_{\text{IPC}}} + 1 \right) \left(\frac{PR_{\text{HPC}}^{\frac{\gamma-1}{\gamma}} - 1}{\eta_{\text{HPC}}} + 1 \right) - 1} \quad (5)$$

where PR_{IPC} , PR_{HPC} , η_{IPC} , and η_{HPC} are pressure ratios and efficiencies of the two compressors; ω is the total pressure loss in the duct (as a fraction of the inlet total pressure); and γ is the ratio of specific heats for air. More details are given in [27,28].

Table 1 Orthogonal polynomials from the Askey scheme [11]

Random variable	Polynomial chaos basis
<i>Continuous</i>	
Gaussian	Hermite
Gamma	Laguerre
Beta	Jacobi
Uniform	Legendre
<i>Discrete</i>	
Poisson	Charlier
Binomial	Krawtchouk
Negative Binomial	Meixner
Hypergeometric	Hahn

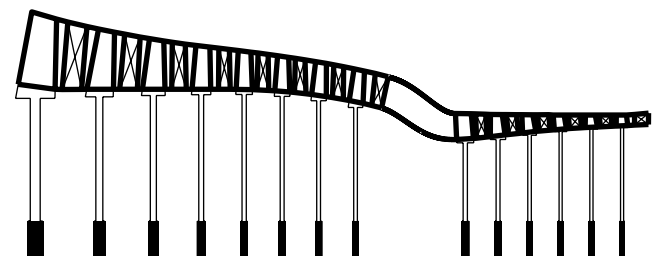


Fig. 2 A schematic meridional view of a core compression system (IPC, duct, and HPC).

Methodology

A review of the main methods available for uncertainty propagation in physical systems was given in the Introduction. The choice of the most appropriate approach to uncertainty quantification (or performance variability analysis) depends both on the specific system under consideration and on the computational resources available; because of the length of the compressor working lines, methods based on the evaluation of the objective function's derivatives (such as sensitivity derivatives and moment methods) are unlikely to provide reliable estimations. If limited information on the relative importance of the different power settings is available, interval analysis is probably the best approach, whereas if a probability density function of the operating point's variation can be estimated, MCS can provide detailed information at a higher computational cost. In the presence of an already complex system, a strategy for reducing the cost of each robustness analysis must be devised. Response surfaces are frequently used to reduce the function evaluation cost and increase the efficiency of the Monte Carlo estimation; PC offers an alternative approach to evaluating performance variation based on a stochastic formulation of the governing equations.

Uncertainty Quantification

As with other aerodynamic metrics, compressor performance is generally expressed in nondimensional (or corrected) terms: the compressor map reports pressure ratio and efficiency as a function of the nondimensional mass flow for several values of constant

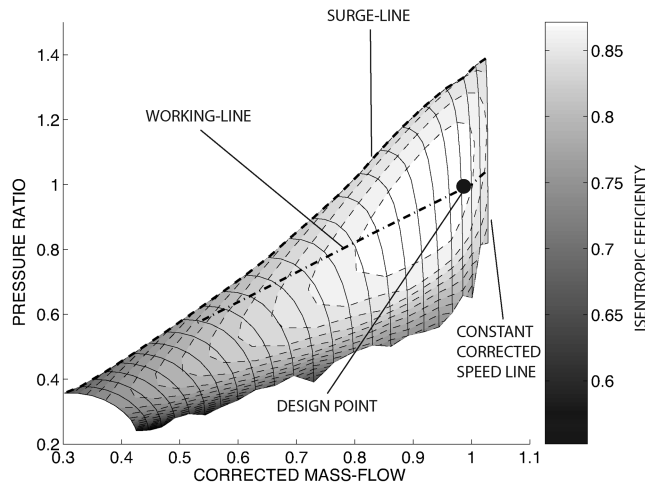


Fig. 3 Typical compressor map: pressure ratio as a function of corrected mass flow is shown for several constant corrected speed lines together with isentropic efficiency contours.

nondimensional speed. More details on the derivation of these nondimensional groups, the generation of compressor maps, and the reasons for their specific form can be found in a number of specialized texts [29,30].

Figure 3 shows the compressor map of a generic core compressor. The most important features are the constant corrected speed lines (extending from surge to choke); the surge line, which represents the location of surge (or rotating stall at low rotational speeds) at different rotational speeds because of excessive flow separation due to the increased flow incidence on the blade at reduced mass flows; and the working line, which represents the locus of stable (or nontransitional) compressor operation at the different rotational speeds. Excursions from working-line operation happen during acceleration/deceleration or because of power offtake or air bleed.

Determination of the Working Line

The working line is the locus of stable operation of the compressor (which happens when compressor and turbine mounted on the same shaft have the same rotational speed, air mass flow, and power produced/required). The determination of the working line for any of the engine components (generally known as engine matching) is typically an iterative process (each component's operation is influenced mutually by other engine components). The operation of a compressor is greatly influenced by the turbine mounted on the same shaft. Detailed derivation is omitted:

$$\begin{cases} \text{PR}_{\text{IPC}} = (1 + k_1 \frac{T_{0,4}}{T_{0,2}} \eta_{\text{LPC}})^{\frac{\gamma}{\gamma-1}} \\ \bar{m}_{\text{IPC}} = k_2 \text{PR}_{\text{IPC}} \text{PR}_{\text{HPC}} \sqrt{\frac{T_{0,2}}{T_{0,4}}} \\ \text{PR}_{\text{HPC}} = (1 + k_3 \frac{T_{0,4}}{T_{0,25}} \eta_{\text{HPC}})^{\frac{\gamma}{\gamma-1}} \\ \bar{m}_{\text{HPC}} = k_4 \text{PR}_{\text{HPC}} \sqrt{\frac{T_{0,25}}{T_{0,4}}} \end{cases} \quad (6)$$

where P_0 and T_0 represent stagnation pressure and temperature; \bar{m} is the pseudo-nondimensional mass flow; $\bar{m} = \dot{m} \sqrt{T_0} / P_0$, with \dot{m} being the air mass flow rate (dimensional); η_{LPC} and η_{HPC} are the isentropic efficiencies of the two compressors; and γ is the ratio of specific heats. The numbered subscripts correspond to states at entry to and exit from the components shown schematically in Fig. 4. Several assumptions (constant mass flow through the system, constant power offtake, choked turbines, constant turbine efficiencies, and constant nozzle areas) were made during this derivation. An iterative process is required, since both pressure ratios and nondimensional mass flows are dependent on the compressors' isentropic efficiencies, which are in turn functions of pressure ratios and nondimensional mass flows. The operating point thus depends (for a given system) only on the ratio $T_{0,4}/T_{0,2}$ (a function of the fuel flow or engine throttle), which can be regarded as the control variable of the system.

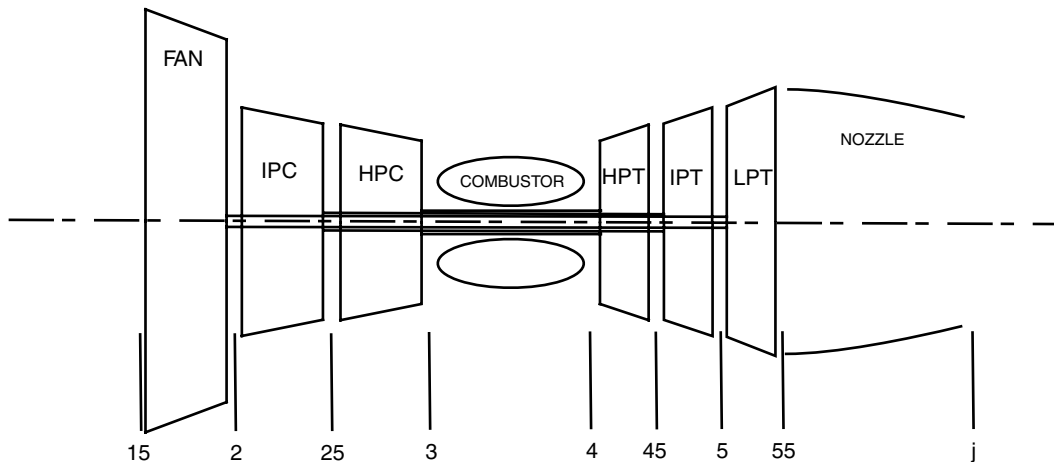


Fig. 4 Schematic of a three-spool gas turbine.

Offdesign Operational Limits

The design-point value for the ratio $T_{0,4}/T_{0,2}$ can be determined from the design-point performance, whereas excursions from this value depend on the engine and compressor operational limits. The design point is generally much closer to the maximum $T_{0,4}/T_{0,2}$, established by the maximum-allowable turbine entry temperature and compressor rotational speed, than to its minimum, which then represents the most dangerous condition from an aerodynamic point of view [30]. The minimum value is normally encountered during engine idling operations (during descent) and can be calculated based on the blowout air–fuel ratio (a typical value for aircraft engine fuels is 250 [31]). The temperature change in the combustion process can be calculated as a function of the air–fuel ratio and the fuel lower calorific value H_v (43 MJ/kg is a typical value for aircraft fuels):

$$\Delta T_{\text{comb}} = \frac{\dot{m}_{\text{fuel}} H_v}{\dot{m} c_p} \quad (7)$$

The minimum combustion temperature rise can be calculated from Eq. (7) and the minimum value for the ratio $T_{0,4}/T_{0,2}$ can be found by imposing the condition

$$\frac{T_{0,4}}{T_{0,2}} \geq \frac{T_{0,3} + \Delta T_{\text{comb, min}}}{T_{0,2}} = \left(\frac{T_{0,4}}{T_{0,2}} \right)_{\text{min}} = f(\text{PR}_{\text{IPC}}, \text{PR}_{\text{HPC}}, \eta_{\text{IPC}}, \eta_{\text{HPC}}) \quad (8)$$

Uncertainty Propagation: Polynomial Chaos

If the PDF of the control variable $T_{0,4}/T_{0,2}$ is available, PC offers a means of calculating high-order information (mean, variance, and successive moments) at a much reduced cost compared with MCS. Wiener [7] employed Hermite polynomials in terms of Gaussian random variables to express stochastic processes with finite variance. This approach is particularly efficient when the input uncertainties are Gaussian-distributed, meaning that they can be expressed through a first-order Hermite chaos (HC) expansion. Lucor et al. [10] demonstrated that an exponential convergence rate can be achieved in this case for a number of test problems, whereas for differently distributed input uncertainties, the convergence rate may be substantially slower.

An extension of the HC expansion (named Wiener–Askey polynomial chaos) was proposed by Xiu and Karniadakis [11] to deal with more general random inputs more efficiently. The underlying concept remains the same (expansion of the generic random process through a set of orthogonal polynomials), but the Hermite polynomials basis is replaced by a generic basis of orthogonal polynomials. A random process $Y(\theta)$ can still be expressed as

$$Y(\theta) = c_0 I_0 + \sum_{i_1=1}^{\infty} c_{i_1} I_1(\xi_{i_1}(\theta)) + \sum_{i_1=1}^{\infty} \sum_{i_2=1}^{i_1} c_{i_1 i_2} I_2(\xi_{i_1}(\theta), \xi_{i_2}(\theta)) + \sum_{i_1=1}^{\infty} \sum_{i_2=1}^{i_1} \sum_{i_3=1}^{i_2} c_{i_1 i_2 i_3} I_3(\xi_{i_1}(\theta), \xi_{i_2}(\theta), \xi_{i_3}(\theta)) + \dots \quad (9)$$

where $I_n(\xi_{i_1}(\theta), \dots, \xi_{i_n}(\theta))$ represents the Wiener–Askey polynomial of order n in terms of the random vector $\xi = (\xi_{i_1}, \dots, \xi_{i_n})$. The polynomials I_n now are not restricted to the Hermite polynomials but can be any orthogonal polynomials. For notational convenience, Eq. (9) can be rewritten as

$$Y(\theta) = \sum_{j=0}^{\infty} \hat{c}_j \Phi_j(\xi) \quad (10)$$

where there is a one-to-one correspondence between the polynomials $I_n(\xi_{i_1}, \dots, \xi_{i_n})$ and $\Phi_j(\xi)$ and between the coefficients \hat{c}_j and c_{i_1, \dots, i_n} . These polynomials are again orthogonal, so

$$\langle \Phi_i \Phi_j \rangle = \langle \Phi_i^2 \rangle \delta_{ij} \quad (11)$$

where δ_{ij} is the Kronecker delta and $\langle \cdot, \cdot \rangle$ denotes the ensemble average. This is the inner product in the Hilbert space of the random variables:

$$\langle f(\xi) g(\xi) \rangle = \int f(\xi) g(\xi) W(\xi) d\xi \quad (12)$$

In determining the Hilbert space inner product, $W(\xi)$ is the weighting function corresponding to the PC basis Φ_i .

The PC basis and supporting distribution can be chosen from the Askey scheme (see Table 1) as most appropriate for the given input uncertainty distribution; this can allow (as in the case of Gaussian distributions and HC) certain input uncertainties to be expressed exactly through a first-order expansion, simplifying the task of solving the stochastic differential equations governing the problem and improving the accuracy of the solution. With this approach, Xiu and Karniadakis [11] achieved exponential convergence for a number of different input distributions, for the same test problems already used by Lucor et al. [10].

Nonintrusive Polynomial Chaos

Even though PC has been applied successfully to the solution of a wide range of problems, its application to the analysis of complex systems can be far from straightforward. Appropriate modification of the equations governing the system behavior can be time-consuming and the implementation of PC can be nontrivial. Modern engineering design involves a large number of disciplines and quite often relies on third-party software products, the modification of which to suit the needs of the PC approach is frequently out of the question. A nonintrusive alternative has been developed based on the observation that the coefficients of the different modes can be obtained by projecting deterministic computations onto the PC basis [32]:

$$\hat{c}_i = \frac{1}{\langle \Phi_i^2 \rangle} \int d\xi_1 \dots \int d\xi_N Y(\xi) \Phi_i(\xi) W(\xi) \quad (13)$$

As $Y(\xi)$ and $\Phi_i(\xi)$ are both polynomials (Φ_i is a polynomial by definition and the Cameron–Martin theorem ensures the convergence of the Fourier–Askey representation of any functional with finite variance to the functional itself [8]), the above integral can be calculated exactly through a Gaussian quadrature formula:

$$\hat{c}_i = \frac{1}{\langle \Phi_i^2 \rangle} \sum_{n_1=1}^{N_0} \dots \sum_{n_N=1}^{N_0} Y(\xi_{n_1}, \dots, \xi_{n_N}) \Phi_i(\xi_{n_1}, \dots, \xi_{n_N}) \prod_{k=1}^N w_{n_k} \quad (14)$$

where the couples (ξ_k, w_k) represent the one-dimensional Gaussian quadrature points and weights. This formula is exact when the integrand is a polynomial of degree less than or equal to $2N_0 - 1$ [33]. The quadrature points are the zeros of the orthogonal polynomial of degree N_0 and the weights can be calculated as

$$w_k = \frac{1}{[\phi'_{N_0}(\xi_k)]^2} \int_{-\infty}^{+\infty} W(\xi) \left[\frac{\phi_{N_0}(\xi)}{\xi - \xi_k} \right]^2 d\xi \quad (15)$$

where $\phi'_{N_0}(\xi_k)$ is the first-order derivative of the orthogonal polynomial of order n at quadrature point ξ_k .

Equation (14) assumes the use of a tensor product of one-dimensional quadrature rules to approximate the multidimensional integral in Eq. (13). The accuracy of the method is clearly a function of N_0 ; assuming the functional $Y(\xi)$ to be well-approximated (in relation to the requirements of the specific application) by a PC expansion of order p , a multidimensional quadrature of order $(p+1)$ will be appropriate for the nonintrusive polynomial chaos (NIPC) approach. It is important to note that a quadrature of order $(p+1)$ does not ensure that the PC coefficients of order less than or equal to p will be calculated exactly, if the PC expansion of order p cannot capture the system response $Y(\xi)$. Similarly, an intrusive formulation of order p does not ensure the first p coefficients will be calculated accurately, due to the coupling of the equations in the corresponding mathematical system (for nonlinear problems).

If $N_0 = p + 1$ and a tensor product quadrature is used, the number of deterministic calculations required by the NIPC approach is equal to $(p + 1)^N$, which is always greater than the $(p + N)!/p!N!$ calculations required by intrusive PC [32] (N is the number of random dimensions and p is the chaos order). This comparison does not take into account the particular structure of the mathematical system of equations deriving from the application of an intrusive PC formulation, which might be exploited by a solver, effectively reducing the cost of the method. Similarly, the comparison does not take into account the memory overload that might be caused by the need to store a larger number of unknowns (corresponding to the coefficients of the PC expansion). Nevertheless, the possibility of treating the analysis software as a black box is an advantage of the NIPC approach. Alternative methods can be used to reduce the number of deterministic simulations required: sparse-grid collocations are a particularly efficient example and their use will be discussed later.

Nonstandard Distributions

As noted, the Cameron–Martin theorem [8] ensures the possibility of using HC to represent any second-order process. In principle, any set of orthogonal polynomials can be used to express any distribution. Choosing the weighting function to match the random variable's input distribution (and choosing the PC basis as a consequence) has the advantage that the input random variable can be expressed exactly as a first-order expansion with respect to the PC basis, simplifying the computations and, more important, improving the convergence of the method. In the case of a nonstandard distribution (or if, for any reason, a particular set of orthogonal polynomials is preferred) the input variable needs to be expressed as a function of the support variable (or, equivalently, the coefficients of its expansion in terms of the elements of the PC basis need to be determined). As for NIPC, the coefficients can be obtained by a projection of the generic input variable k onto the PC basis:

$$k_i = \frac{\langle k \Phi_i \rangle}{\langle \Phi_i^2 \rangle} = \frac{1}{\langle \Phi_i^2 \rangle} \int k \Phi_i(\xi) W(\xi) d\xi \quad (16)$$

The main assumption here is that the variables k and ξ are fully correlated (i.e., a univocal relation exists between ξ and k) [11]. In this form, the integral in Eq. (16) cannot be evaluated, as the variables k and ξ belong to two different probability spaces. By taking a support variable z , uniformly distributed in the interval (0,1), it is possible to apply a variable transformation such as

$$dz = f(k)dk = dF(k) \quad dz = g(\xi)d\xi = dG(\xi) \quad (17)$$

where $f(k)$ and $g(\xi)$ are the PDFs of k and ξ , respectively, and $F(k)$ and $G(\xi)$ are their cumulative distribution functions. It follows that

$$z = \int_{-\infty}^k f(t) dt = F(k) \quad z = \int_{-\infty}^{\xi} g(t) dt = G(\xi) \quad (18)$$

and

$$k = F^{-1}(z) = h(z) \quad \xi = G^{-1}(z) = l(z) \quad (19)$$

Equation (16) thus becomes

$$k_i = \frac{1}{\langle \Phi_i^2 \rangle} \int_a^b k \Phi_i(\xi) W(\xi) d\xi = \frac{1}{\langle \Phi_i^2 \rangle} \int_0^1 h(z) \Phi_i(l(z)) dz \quad (20)$$

The inverses of the cumulative distribution functions for some common distributions are known [11]. Alternatively, they can be calculated numerically given the corresponding PDFs.

Consider an input variable with a nonstandard multimodal PDF. A fourth-order polynomial has been chosen for simplicity, but the conclusions would not change for a different PDF:

$$f(k) = 18.2342k - 95.2432k^2 + 164.5764k^3 - 87.5675k^4 \quad (21)$$

for $0 \leq k \leq 1$

An expansion in terms of standard orthogonal polynomials from the Askey scheme is still possible, but the order required becomes higher and this would necessitate an even higher PC order in the solution of the system of equations that describe the problem or a higher quadrature formula if a nonintrusive strategy is adopted, with the risk of incurring large truncation errors. Figure 5 shows the results for expansions using Legendre polynomials in terms of a uniformly distributed support random variable: not only is the order of the polynomial expansion required high (although a satisfactory level of approximation can be reached, it requires at least a 15th-order expansion), but the approximation itself suffers from the well-known overfitting problem typical of high-order polynomials [33]. An alternative approach could consist of dividing the PDF in two parts, expressing each of them as a separate PC expansion and separately propagating the two distributions, but this solution would clearly also involve a large degree of approximation and require the solution of two stochastic systems.

Constructing Generic Orthogonal Polynomials

A more efficient approach for handling nonstandard distributions is to determine the set of orthogonal polynomials with respect to the generic distribution (which has been normalized here to between 0 and 1, for simplicity). A detailed review of the main techniques available for generating orthogonal polynomials (based on the Stieltjes procedure and the Chebyshev algorithm) with respect to a generic probability measure is given by Gautschi [34].

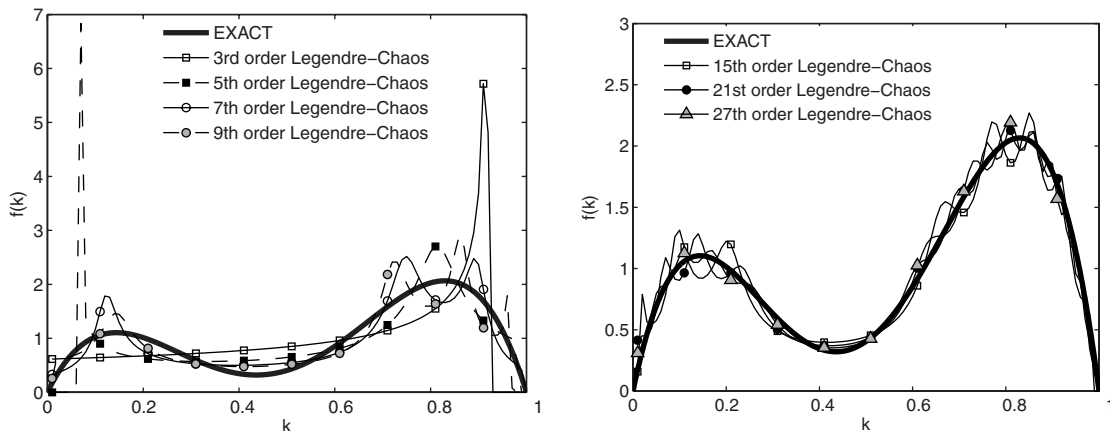


Fig. 5 Approximation of a nonstandard PDF through Legendre chaos.

A generic expression for an orthogonal polynomial of order m is

$$P_m(\xi) = \sum_{j=0}^m b_{m,j} \xi^j \quad (22)$$

The orthogonality condition can be expressed as

$$\int_0^1 P_m(\xi) W(\xi) \xi^k d\xi = 0 \quad \text{for } k = 0, \dots, m-1 \quad (23)$$

The integral in Eq. (23) simplifies if the weighting function $W(\xi)$ can be expressed as a polynomial (or can be calculated numerically when dealing with a nonpolynomial PDF):

$$W(\xi) = \sum_{i=0}^n a_i \xi^i \quad (24)$$

In this case,

$$\int_0^1 P_m(\xi) W(\xi) \xi^k d\xi = \int_0^1 \sum_{j=0}^m b_{m,j} \xi^j \sum_{i=0}^n a_i \xi^i \xi^k d\xi \quad (25)$$

for $k = 0, \dots, m-1$

The integrals in Eq. (25) give the following conditions:

$$\sum_{j=0}^m b_{m,j} \sum_{i=0}^n \frac{a_i}{i+j+k+1} = 0 \quad \text{for } k = 0, \dots, m-1 \quad (26)$$

The system in Eq. (26) has m equations for $m+1$ unknowns (the coefficients of P_m). The remaining condition can come from the choice of a value for the intercept ($b_{m,0} = 1$, for example). The coefficients of the orthogonal polynomial of degree m can thus be derived by solving the following system:

$$\begin{bmatrix} \sum_{i=0}^n \frac{a_i}{i+1} & \sum_{i=0}^n \frac{a_i}{i+2} & \cdots & \sum_{i=0}^n \frac{a_i}{i+m+1} \\ \sum_{i=0}^n \frac{a_i}{i+2} & \sum_{i=0}^n \frac{a_i}{i+3} & \cdots & \sum_{i=0}^n \frac{a_i}{i+m+2} \\ \vdots & \vdots & \ddots & \vdots \\ \sum_{i=0}^n \frac{a_i}{i+m} & \sum_{i=0}^n \frac{a_i}{i+m+1} & \cdots & \sum_{i=0}^n \frac{a_i}{i+m+1} \\ 1 & 0 & \cdots & 0 \end{bmatrix} \begin{bmatrix} b_{m,0} \\ b_{m,1} \\ \vdots \\ b_{m,m} \end{bmatrix} = \begin{bmatrix} 0 \\ 0 \\ \vdots \\ 0 \\ 1 \end{bmatrix} \quad (27)$$

The accuracy of the method depends on the numerical condition of the matrix in Eq. (27). The condition of this matrix grows rapidly with the order of the polynomial in question (10^8 for a 10th-order polynomial). This is acceptable in the current application (the error being the product of the matrix condition and machine epsilon, which is of the order of 10^{-19} in double-precision arithmetic), but can become a problem if higher-order expansions are sought.

An alternative approach is to use the Stieltjes procedure [35] to generate the one-dimensional basis of orthogonal polynomials. This method is based on the three-term recurrence relation for orthogonal monic polynomials:

$$P_{m+1}(\xi) = (\xi - c_1)P_m(\xi) - c_2P_{m-1}(\xi) \quad (28)$$

where

$$c_1 = \frac{\int \xi P_m^2(\xi) w(\xi) d\xi}{\int P_m^2(\xi) w(\xi) d\xi}, \quad c_2 = \frac{\int P_m^2(\xi) w(\xi) d\xi}{\int P_{m-1}^2(\xi) w(\xi) d\xi} \quad (29)$$

The corresponding system remains well-conditioned for high-order polynomials, as demonstrated in [34]. With the assumption in Eq. (24), the calculation of the above coefficients can be simplified:

$$c_1 = \frac{\sum_{i=0}^m \sum_{j=0}^m \sum_{k=0}^n \frac{b_{m,i} b_{m,j} a_k}{i+j+k+2}}{\sum_{i=0}^m \sum_{j=0}^m \sum_{k=0}^n \frac{b_{m,i} b_{m,j} a_k}{i+j+k+1}} \quad (30)$$

$$c_2 = \frac{\sum_{i=0}^m \sum_{j=0}^m \sum_{k=0}^n \frac{b_{m,i} b_{m,j} a_k}{i+j+k+1}}{\sum_{i=0}^{m-1} \sum_{j=0}^{m-1} \sum_{k=0}^n \frac{b_{m-1,i} b_{m-1,j} a_k}{i+j+k+1}}$$

To further simplify the calculations (and the results), it is convenient to normalize the polynomials thus obtained. This can be achieved by dividing the coefficients of the polynomial of degree m by h_m , where

$$h_m^2 = \langle P_m^2 \rangle = \int_0^1 \sum_{i=0}^m \sum_{j=0}^m \sum_{k=0}^n b_{m,i} b_{m,j} a_k \xi^{i+j+k} d\xi$$

$$= \sum_{i=0}^m \sum_{j=0}^m \sum_{k=0}^n \frac{b_{m,i} b_{m,j} a_k}{i+j+k+1} \quad (31)$$

We denote $P_m^* = P_m/h_m$ as the orthonormal polynomial of degree m (with coefficients $b_{m,i}^*$, for $i = 0, \dots, m$). All the bases of orthogonal polynomials obey a recurrence relation of the type [33]

$$P_{m+1}(\xi) = (A_m \xi + B_m)P_m(\xi) - C_m P_{m-1}(\xi) \quad (32)$$

with

$$A_m = \frac{b_{m+1,m+1}}{b_{m,m}}, \quad B_m = A_m \left(\frac{b_{m+1,m}}{b_{m+1,m+1}} - \frac{b_{m,m-1}}{b_{m,m}} \right)$$

$$C_m = \frac{A_m}{A_{m-1}} \frac{h_m}{h_{m-1}}$$

For orthonormal polynomials, Eq. (32) becomes

$$P_{m+1}^*(\xi) = (A_m^* \xi + B_m^*)P_m^*(\xi) - C_m^* P_{m-1}^*(\xi) \quad (33)$$

with

$$A_m^* = \frac{b_{m+1,m+1}^*}{b_{m,m}^*}, \quad B_m^* = A_m^* \left(\frac{b_{m+1,m}^*}{b_{m+1,m+1}^*} - \frac{b_{m,m-1}^*}{b_{m,m}^*} \right)$$

$$C_m^* = \frac{A_m^*}{A_{m-1}^*}$$

It is possible to recast Eq. (33) in the following form:

$$\xi P_m^*(\xi) = \frac{1}{A_m^*} P_{m+1}^*(\xi) - \frac{B_m^*}{A_m^*} P_m^*(\xi) + \frac{C_m^*}{A_m^*} P_{m-1}^*(\xi) = \alpha_m P_{m-1}^*(\xi)$$

$$+ \beta_m P_m^*(\xi) + \gamma_m P_{m+1}^*(\xi) \quad (34)$$

where

$$\alpha_m = \frac{C_m^*}{A_m^*} = \frac{1}{A_{m-1}^*} = \frac{b_{m-1,m-1}^*}{b_{m,m}^*}$$

$$\beta_m = -\frac{B_m^*}{A_m^*} = -\left(\frac{b_{m+1,m}^*}{b_{m+1,m+1}^*} - \frac{b_{m,m-1}^*}{b_{m,m}^*} \right) \quad \gamma_m = \frac{1}{A_m^*} = \frac{b_{m,m}^*}{b_{m+1,m+1}^*}$$

Equation (34) further simplifies to

$$\xi P_m^*(\xi) = \gamma_{m-1} P_{m-1}^*(\xi) + \beta_m P_m^*(\xi) + \gamma_m P_{m+1}^*(\xi) \quad (35)$$

where $\gamma_{-1} = 0$. In matrix form, Eq. (35) reads

Table 2 System of orthonormal polynomials

Order	P_i^*	$\langle (P_i^*)^2 \rangle$
0	1	1
1	$2.0293 - 3.4512\xi$	1
2	$2.6955 - 16.3218\xi + 16.0617\xi^2$	1
3	$4.0995 - 42.7907\xi + 98.4216\xi^2 - 62.8152\xi^3$	1
4	$5.0015 - 81.4621\xi + 347.0134\xi^2 - 524.4300\xi^3 + 258.0990\xi^4$	1
5	$6.5207 - 149.9490\xi + 963.9440\xi^2 - 2444.9253\xi^3 + 2661.0726\xi^4 - 1041.7694\xi^5$	1
6	$7.7384 - 237.3649\xi + 2133.9160\xi^2 - 8103.0401\xi^3 + 14720.2905\xi^4 - 12687.9273\xi^5 + 4172.7058\xi^6$	1

$$\begin{aligned}
 & \begin{bmatrix} P_0^*(\xi) \\ P_1^*(\xi) \\ P_2^*(\xi) \\ P_3^*(\xi) \\ \vdots \\ P_{G-2}^*(\xi) \\ P_{G-1}^*(\xi) \end{bmatrix} = \begin{bmatrix} \beta_0 & \gamma_0 & 0 & 0 & \cdots & 0 & 0 \\ \gamma_0 & \beta_1 & \gamma_1 & 0 & \cdots & 0 & 0 \\ 0 & \gamma_1 & \beta_2 & \gamma_2 & \cdots & 0 & 0 \\ 0 & 0 & \gamma_2 & \beta_3 & \cdots & 0 & 0 \\ \vdots & \vdots & \vdots & \vdots & \vdots & \vdots & \vdots \\ 0 & 0 & 0 & 0 & \cdots & \beta_{G-2} & \gamma_{G-2} \\ 0 & 0 & 0 & 0 & \cdots & \gamma_{G-2} & \beta_{G-1} \end{bmatrix} \\
 & \times \begin{bmatrix} P_0^*(\xi) \\ P_1^*(\xi) \\ P_2^*(\xi) \\ P_3^*(\xi) \\ \vdots \\ P_{G-2}^*(\xi) \\ P_{G-1}^*(\xi) \end{bmatrix} + \begin{bmatrix} 0 \\ 0 \\ 0 \\ 0 \\ \vdots \\ 0 \\ \gamma_{G-1} P_G^*(\xi) \end{bmatrix} \quad (36)
 \end{aligned}$$

This means that to find the roots of the orthonormal polynomial of degree G , we need to solve the system

$$\xi p(\xi) = \mathbf{B} p(\xi) \quad (37)$$

which is an eigenvalues-eigenvectors problem. The eigenvalues of matrix \mathbf{B} will correspond to the roots of the orthonormal polynomial $P_G(\xi)$ of degree G and the eigenvectors will correspond to the values of the polynomials of degree less than G (apart from a multiplicative constant that can be determined by recalling that $P_0(\xi) = 1$) at the points defined by the corresponding eigenvalues. The roots of the orthonormal polynomial of order G correspond to the quadrature points for the Gaussian quadrature formula of order G . The weights can be determined by

$$w_i(\xi_i) = \frac{1}{\sum_{j=0}^{G-1} [P_j(\xi_i)]^2} \quad (38)$$

as given in [36].

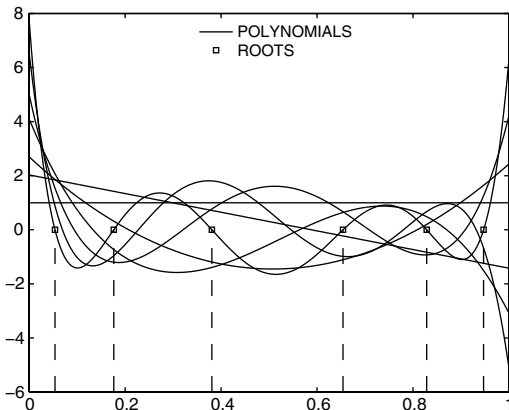


Fig. 6 Orthonormal polynomials up to degree 6, with quadrature-point values.

Table 3 Roots and weights of a sixth-order quadrature

Root ξ_i	Weight w_i	P_0	P_1	P_2	P_3	P_4	P_5
0.0538	0.0652	1.0000	1.8436	1.8638	2.0723	1.5435	0.8841
0.1763	0.1665	1.0000	1.4208	0.3170	-0.7299	-1.1989	-0.9582
0.3808	0.1146	1.0000	0.7150	-1.1908	-1.3917	0.7695	1.8071
0.6542	0.2437	1.0000	-0.2284	-1.1083	0.6407	0.6665	-0.9837
0.8285	0.3053	1.0000	-0.8299	0.1974	0.4829	-0.9285	0.6723
0.9471	0.1046	1.0000	-1.2394	1.6445	-1.5083	1.2597	-0.6773

Consider again the same polynomial PDF of Fig. 5. The basis of orthogonal polynomials with respect to this PDF can be determined by imposing the orthogonality condition in Eq. (27). The resulting orthonormal polynomials are reported in Table 2 and in Fig. 6 (graphically).

A first-order expansion in terms of this new set of orthonormal polynomials (with respect to a weighting function with the same distribution as $f(x)$) will express the input distribution exactly and simplify its propagation through the system under consideration. The roots of the generic orthonormal polynomial of degree G , the values of the orthonormal polynomials of degree less than G at the quadrature points, and the weights can now all be calculated (Table 3).

Once the PC expansion has been determined, the relevant statistics can be rapidly calculated. Only mean, variance, and third-order moment are reported [Eqs. (39) et seq.]:

$$\mu = \int_0^1 \sum_{i=0}^p y_i P_i^*(\xi) W(\xi) d\xi = y_0 \quad (39)$$

$$\sigma^2 = \int_0^1 \left(\sum_{i=1}^p y_i P_i^*(\xi) \right)^2 W(\xi) d\xi = \sum_{i=1}^p y_i^2 \quad (40)$$

$$s^3 = \int_0^1 \left(\sum_{i=1}^p y_i P_i^*(\xi) \right)^3 W(\xi) d\xi = \sum_{i=1}^p \sum_{j=1}^p \sum_{k=1}^p y_i y_j y_k \langle P_i^* P_j^* P_k^* \rangle \quad (41)$$

where

$$Y(\xi) = \sum_{i=0}^p y_i P_i^*(\xi)$$

is the response of the system in terms of the adopted PC expansion, and the triple product $\langle P_i^* P_j^* P_k^* \rangle$ can be calculated as

$$\langle P_i^* P_j^* P_k^* \rangle = \sum_{i_1=0}^i \sum_{i_2=0}^j \sum_{i_3=0}^k \sum_{i_4=0}^n \frac{b_{i,i_1}^* b_{j,i_2}^* b_{k,i_3}^* a_{i_4}}{i_1 + i_2 + i_3 + i_4 + 1} \quad (42)$$

where n is the degree of the weighting function $W(\xi)$ [Eq. (24)].

Results

One-Dimensional Uncertainty

The NIPC approach was applied to the compression system (IPC, duct, and HPC) to evaluate the variability in system efficiency for an input parameter $T_{0,4}/T_{0,2}$ with a PDF as shown in Fig. 5. A

comparison between the PDF obtained with an MCS approach (with 10^6 simulations) and the adaptive PC is presented in Fig. 7, for different PC orders. It is evident how even a third-order PC approach (and therefore four deterministic simulations of the system performance) provides a good approximation for the true PDF of the system response, whereas the results of a fourth-order chaos are almost indistinguishable from the MCS results. The same comparison is presented in Fig. 8 for the Legendre chaos, showing an evident convergence rate deterioration, due to the higher order required to describe the input PDF (see Fig. 5), which translates into an even higher order for the system's response. The PC order required to approximate the system's response $Y(\xi)$ with a given accuracy depends on the relation between Y and the support random variable ξ . Choosing the support variable to match the input uncertainty ($T_{0.4}/T_{0.2}$ in this case) simplifies this relation. This choice also allows the input uncertainty to be captured exactly by the PC approach, rather than approximated as it would be when using any standard basis of orthogonal polynomials from the Askey scheme (Table 1). The error in Fig. 8 therefore has two sources:

- 1) Error is generated in approximating the input uncertainty $T_{0.4}/T_{0.2}$ with a Legendre chaos expansion (see Fig. 5).
- 2) A substantial increase in the order is required to capture the relation between the support variable and the system's response.

The same results are summarized in Fig. 9 in terms of the system response's main moments; the convergence of errors in the mean and variance as the quadrature order increases is shown on a semilog plot, compared with the results obtained using a Gauss–Legendre quadrature, after the nonstandard PDF has been expressed in terms of a uniformly distributed random variable. Errors for mean and variance have been calculated as

$$\epsilon_{\text{mean}} = \left| \frac{\mu - \mu_r}{\mu_r} \right|, \quad \epsilon_{\text{var}} = \left| \frac{\sigma^2 - \sigma_r^2}{\sigma_r^2} \right|$$

where, in the absence of an analytical solution and given the impossibility of obtaining an accurate enough estimate through MCS, the reference values μ_r and σ_r^2 have been chosen as those given by a 10th-order quadrature. The improvements are evident and a quasi-exponential convergence rate is shown, even for the complex problem under consideration.

Monte Carlo simulation is the only method that guarantees to be able to calculate the desired PDF (and then its moments) exactly. In practice, its slow convergence [the error is $\mathcal{O}(1/\sqrt{m})$, where m is the number of simulations] makes its application in already expensive deterministic simulations unrealistic, unless some kind of response surface is used to approximate the function's behavior. Figure 10a reports the convergence of mean and variance with the number of evaluations for a typical MCS (because of the randomness of the method, every MCS will lead to a different convergence history). The values have been nondimensionalized with the results obtained after 10^6 simulations. Figure 10b reports the convergence of the NIPC approach (the values have again been nondimensionalized with the results obtained after 10^6 MCS). The reduction in computational cost is of at least two orders of magnitude.

Multidimensional Uncertainty

In the previous section, the variability in the core compression system performance in the presence of a given PDF for the engine throttle was calculated by treating the ratio $T_{0.4}/T_{0.2}$ as a stochastic variable and using a one-dimensional nonintrusive polynomial chaos

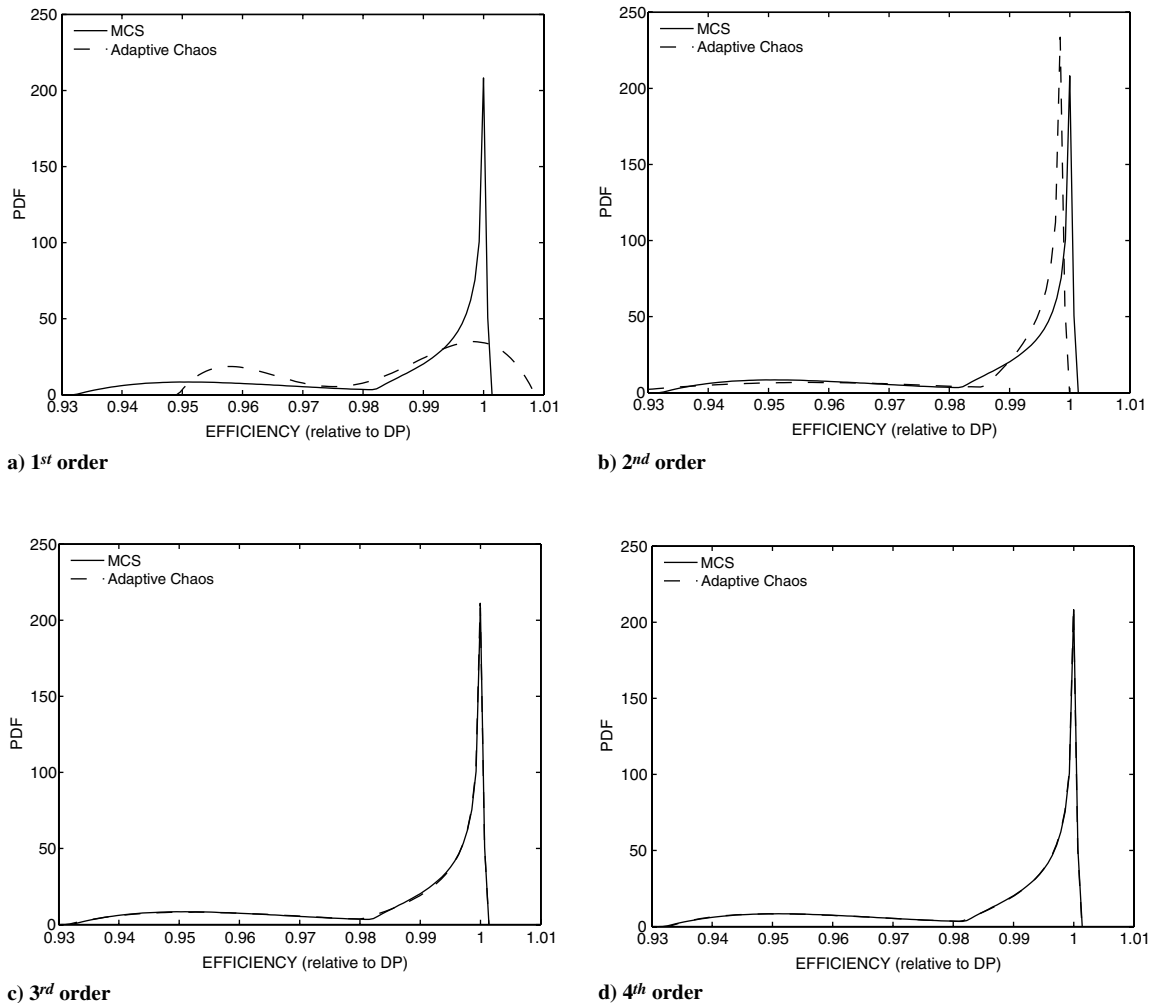


Fig. 7 Comparison between the system efficiency PDF obtained with Monte Carlo simulations and adaptive chaos.

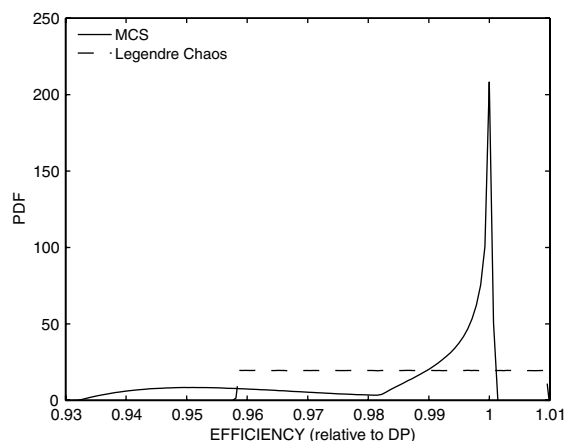
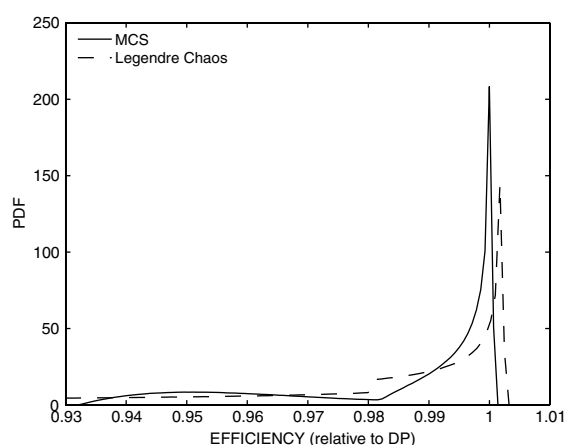
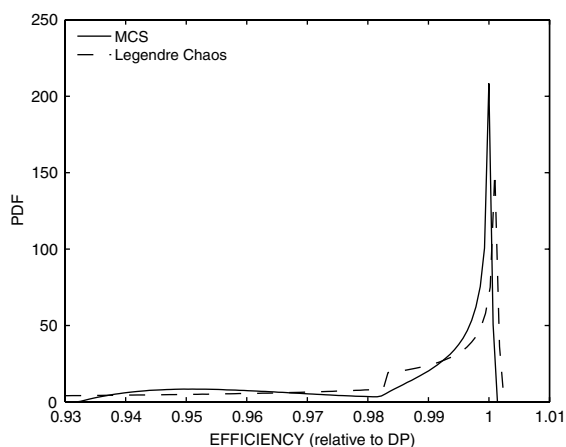
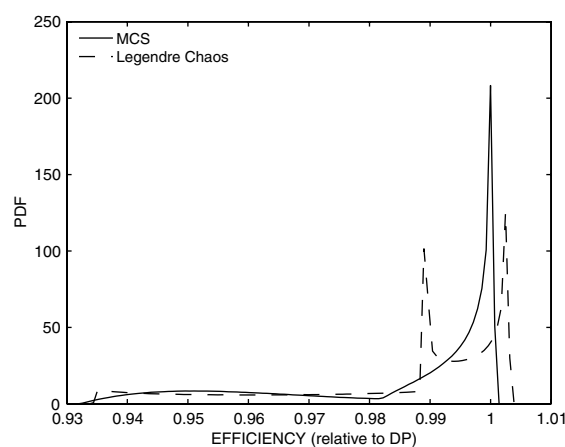
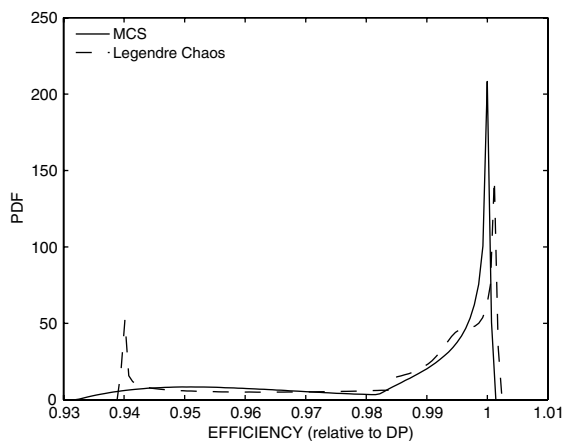
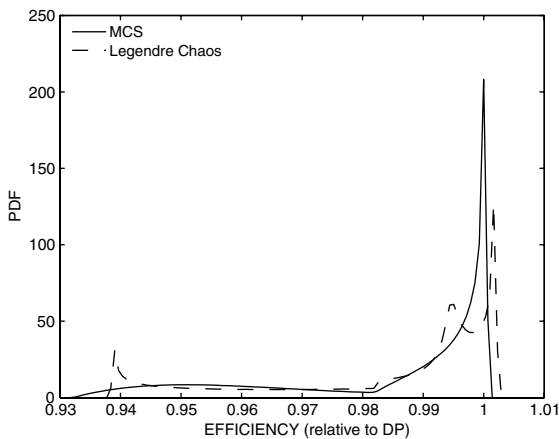
a) 1st orderb) 2nd orderc) 3rd orderd) 4th ordere) 5th orderf) 6th order

Fig. 8 Comparison between the system efficiency PDF obtained with Monte Carlo simulations and Legendre chaos.

approach to propagate the input distribution through the system under consideration. As previously noted, each compressor's operating point depends on the characteristics of other engine components (following compressors and turbines above all). A number of assumptions have been made to calculate the compressors' working lines in Eqs. (6), such as constant mass flow through the system, constant power offtake, constant turbine efficiencies, and choked turbine nozzles. Although some of these assumptions are dictated by a lack of knowledge (turbines' efficiencies and mass flows are a function of their operating points, which can be calculated with an

iterative procedure similar to that adopted for the compressors, given the turbines' characteristics), others such as air bleed and power offtake may, in essence, be independent of the engine throttle.[†] If this

[†]The assumption of independence among the noise factors is necessary to calculate the integral in Eq. (16). In this work we assume engine throttle, power offtake, and air bleed to be independent variables, for simplicity and in view of the difficulty of retrieving real engine data. If this is not the case, the input distributions can be expressed in terms of independent variables through a Karhunen–Loève expansion, as shown by Ghanem and Spanos [9].

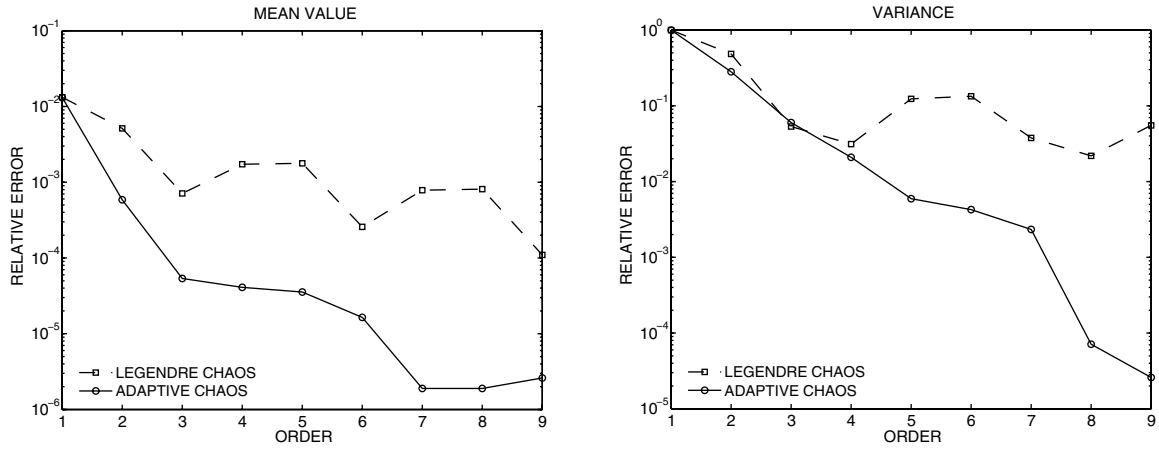


Fig. 9 Convergence of different PC approaches.

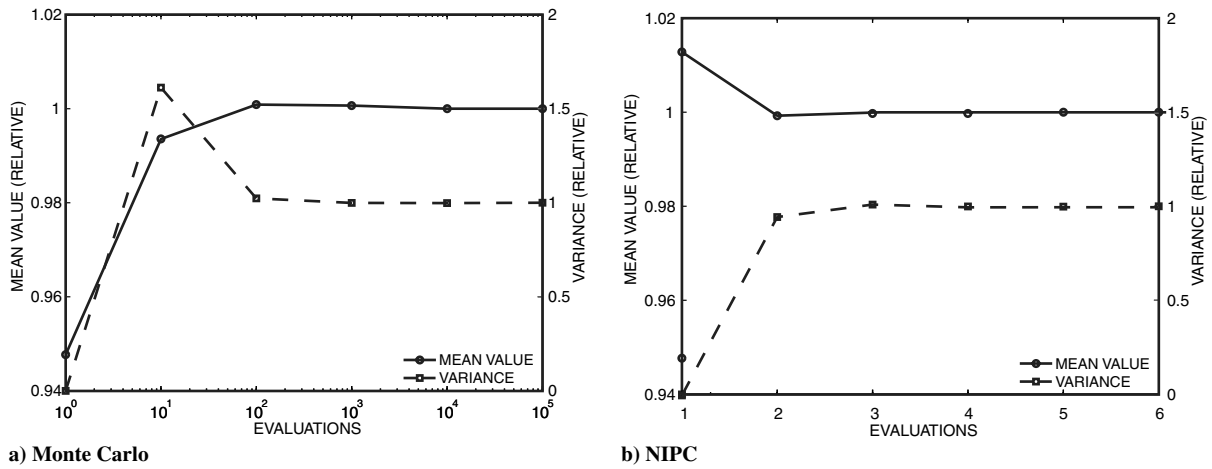


Fig. 10 Comparison of MCS and NIPC convergence.

is the case, it is possible to propagate these additional uncertainties through the system with the NIPC approach. Assuming a fraction of the inlet mass flow to be extracted at the IPC exit and a power offtake from the HPC, Eqs. (6) can be modified as follows:

$$\begin{cases} \text{PR}_{\text{IPC}} = \left(1 + k_1 \frac{\tau_1}{\tau_2} \eta_{\text{LPC}}\right)^{\frac{\gamma}{\gamma-1}} \\ \bar{m}_{\text{IPC}} = k_2 \text{PR}_{\text{IPC}} \text{PR}_{\text{HPC}} \frac{\tau_2}{\sqrt{\tau_1}} \\ \text{PR}_{\text{HPC}} = \left(1 + k_3 \frac{\tau_1}{\tau_3} \frac{T_{0.2}}{T_{0.25}} \eta_{\text{HPC}}\right)^{\frac{\gamma}{\gamma-1}} \\ \bar{m}_{\text{HPC}} = k_4 \text{PR}_{\text{HPC}} \sqrt{\frac{T_{0.25}}{T_{0.2}} \frac{1}{\tau_1}} \end{cases} \quad (43)$$

where $\tau_1 = T_{0.4}/T_{0.2}$, $\tau_2 = \dot{m}_{\text{IPC}}/\dot{m}_{\text{HPC}}$ is the ratio between the mass flow before and after the air bleed, and

$$\tau_3 = \frac{\dot{W}_{\text{HPT}}}{\dot{W}_{\text{HPC}}} = 1 + \frac{\dot{W}_{\text{OT}}}{\dot{W}_{\text{HPC}}}$$

is the ratio between high-pressure turbine work and high-pressure compressor work, a function of the power offtake \dot{W}_{OT} .

The PDFs assumed for the three input random variables (Fig. 11) have been chosen to demonstrate the generality of this approach. Different PDFs could be substituted if available, without requiring any modification to the approach and the software in use.

Support random variables ξ_1 , ξ_2 , and ξ_3 have been chosen with PDFs matching the PDFs of τ_1 , τ_2 , and τ_3 , respectively, but normalized between 0 and 1 to simplify the calculation of the basis of orthonormal polynomials and the relative quadrature rules, allowing the input variables to be expressed as first-order expansions in terms of the corresponding support variable.

The set of orthonormal polynomials calculated based on the given PDFs is used to approximate the functional form between the stochastic system generic output (mass flow, pressure ratio, efficiency, or any other system characteristic), and each of the random inputs. The chaos expansion for a generic response Y takes the form

$$\begin{aligned} Y(\xi_1, \xi_2, \xi_3) = & a_0 \Pi_0 + \sum_{i_1=1}^3 a_{i_1} \Pi_1(\xi_{i_1}) + \sum_{i_1=1}^3 \sum_{i_2=1}^{i_1} a_{i_1, i_2} \Pi_2(\xi_{i_1}, \xi_{i_2}) \\ & + \sum_{i_1=1}^3 \sum_{i_2=1}^{i_1} \sum_{i_3=1}^{i_2} a_{i_1, i_2, i_3} \Pi_3(\xi_{i_1}, \xi_{i_2}, \xi_{i_3}) \\ & + \sum_{i_1=1}^3 \sum_{i_2=1}^{i_1} \sum_{i_3=1}^{i_2} a_{i_1, i_2, i_3} \Pi_4(\xi_{i_1}, \xi_{i_2}, \xi_{i_3}) + \dots \end{aligned} \quad (44)$$

or, if a term-based indexing is used,

$$Y(\xi_1, \xi_2, \xi_3) = \sum_{i=0}^{\infty} y_i \Theta_i(\xi_1, \xi_2, \xi_3) \quad (45)$$

where each of the Θ_i is a multivariate polynomial obtained as a product of the one-dimensional orthonormal polynomials. The summation in Eq. (45) is truncated for practical purposes to a finite order p [for a total of $(p+N)!/p!N!$ terms, with N being the number of uncertain dimensions].

Each of the coefficients of the PC expansion can be obtained by projecting the generic variable on the elements of the PC basis:

$$y_i = \int_{\Omega} Y \Theta_i(\xi) W(\xi) d\xi \quad (46)$$

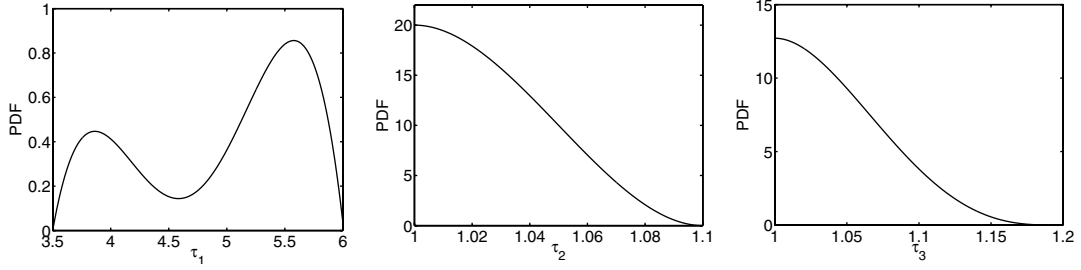


Fig. 11 PDFs for the input uncertainties: engine throttle τ_1 (left), air bleed τ_2 (middle), and power offtake τ_3 (right).

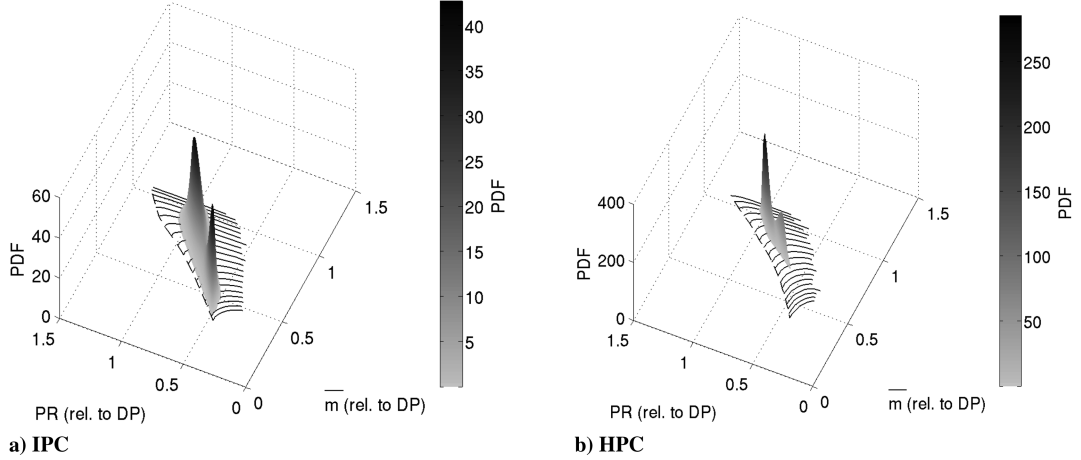


Fig. 12 IPC and HPC maps with probability distributions.

where Ω is the hypercube $[0, 1]^3$, and $W(\xi)$ is the joint probability density function, corresponding to $W_1(\xi_1)W_2(\xi_2)W_3(\xi_3)$ under the assumption of independent random variables.

The integral in Eq. (46) can again be calculated through a quadrature approach; the simplest technique for calculating multi-dimensional integrals is a tensor product of the one-dimensional quadrature rules:

$$y_i = \sum_{i=1}^{N_0} \sum_{j=1}^{N_0} \sum_{k=1}^{N_0} Y(\xi_{1_i}, \xi_{2_j}, \xi_{3_k}) \Theta_i(\xi_{1_i}, \xi_{2_j}, \xi_{3_k}) w_{1_i} w_{2_j} w_{3_k} \quad (47)$$

The use of the Gaussian abscissas (corresponding to the roots of the orthonormal polynomials) and weights is particularly convenient, as it ensures an exact integration of polynomials of degree up to $2N_0 - 1$, with N_0 being the order of the quadrature formula.

Figure 12 shows the joint nondimensional mass-flow/pressure-ratio PDF for both IPC and HPC compressors, together with the compressor map, expressing the probability of each compressor operating at a particular point of the map. Both distributions have

been calculated by means of an NIPC approach, employing a fifth-order quadrature, for a total of 125 system evaluations. The same results are shown in Fig. 13 as contour plots.

Figure 14 shows the convergence of the NIPC approach toward the results obtained with a 10^6 -evaluation MCS. A fourth-order adaptive chaos (125 evaluations) is sufficient to obtain results indistinguishable from those obtained with MCS, whereas even a third-order approach (64 evaluations) ensures a good approximation to the true PDF, at least for practical engineering purposes (the quadrature order N_0 has been chosen equal to the PC order plus one).

Mitigating the Curse of Dimensionality

A full tensor product quadrature formula is an effective approach for calculating multidimensional integrals when the number of dimensions is relatively small, but since the number of collocation points grows exponentially with the number of random dimensions, its effectiveness deteriorates rapidly for larger-dimensionality problems. In contrast, the convergence rate of MCS is only mildly dependent on the number of random uncertainties [37], making it the

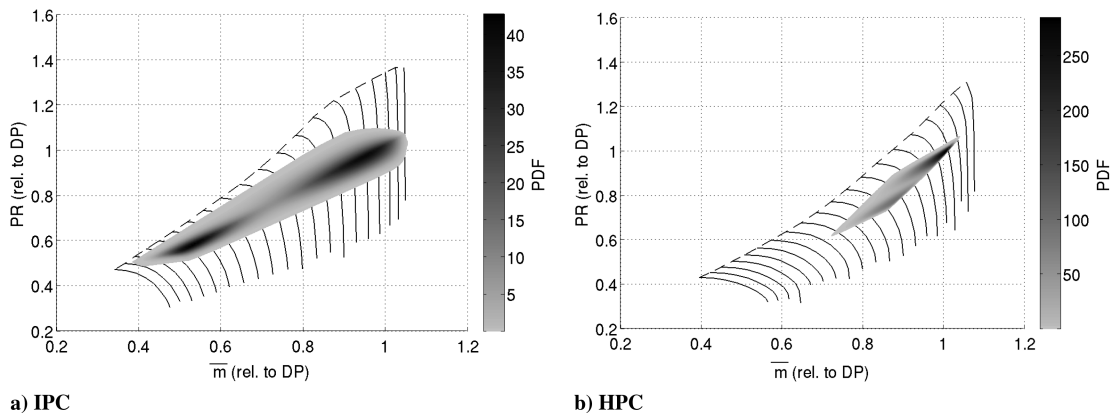


Fig. 13 IPC and HPC maps, with probability contour plots.

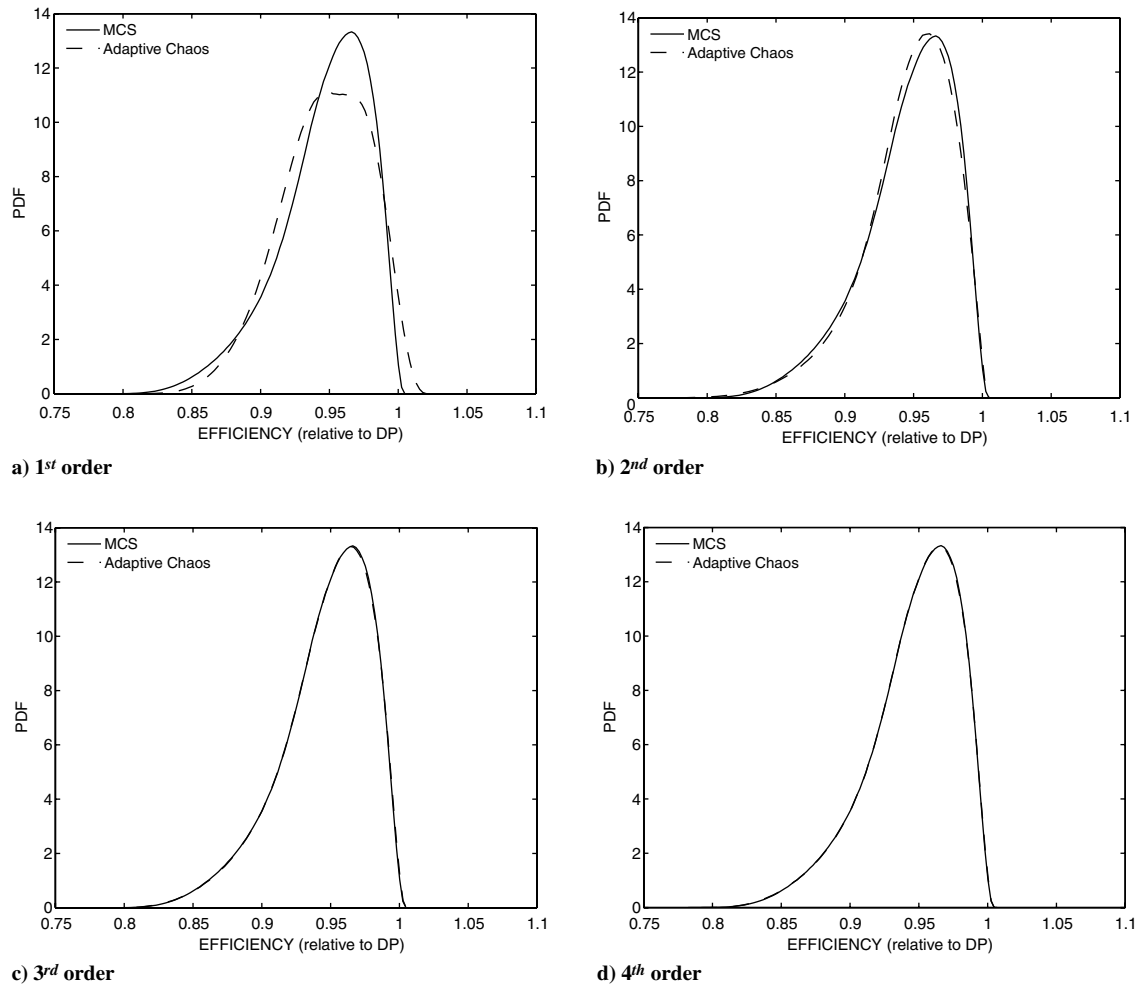


Fig. 14 Comparison between the system efficiency PDF obtained with Monte Carlo simulations and adaptive chaos of increasing order in the presence of three uncertain parameters.

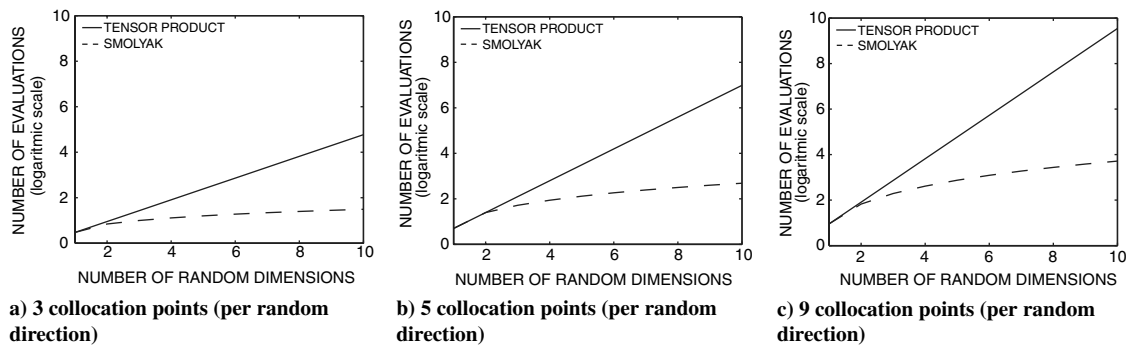


Fig. 15 Comparison of the number of collocation points required by a full tensor grid and by a Smolyak [38] sparse grid.

only sensible approach in problems with a large number of random uncertainties. In practice, if a system is characterized by a large number of input uncertainties, the chances of these being interdependent are often quite high. A Karhunen–Loève expansion can be used to decompose the input multidimensional noise in terms of its principal components** and to isolate the most energetic sources of uncertainty, which can be, in most of the cases, limited to a relatively small number [9].

In problems with a moderately large number of variables, sparse tensor product grids (first proposed by Smolyak [38]) can be used to reduce the number of collocation points, while preserving a high level of accuracy. Nobile et al. [37] proved the effectiveness of sparse-grid

collocation approaches (when compared with MCS) for a stochastic linear elliptic problem in two spatial dimensions with up to 11 independent random variables. A further improvement can be achieved by means of adaptive sparse grids [39,40], where the number of collocation points in each random dimension is chosen adaptively based on the difference between approximations of successive orders.

Figure 15 compares the number of collocation points required by the two NIPC approaches (tensor product quadrature and sparse grids) for different quadrature orders.

Conclusions

A common simplification in engineering design is to consider nominal values for a number of design parameters. Although making complex problems tractable, this approach can lead to products that

**Interdependency among the random variables is also required for the quadrature formula in Eq. (14).

present considerable performance degradation in real-world conditions. In gas turbine design, the different engine modules are usually designed with some specific operating condition in mind (the design point). Although the design point normally represents the most important operating condition (the one the engine spends the most time at), safe and satisfactory operation must be guaranteed at a number of other important points inside the engine performance envelope. In the traditional design approach, offdesign operation is usually considered only at a later stage of the design process. Although guaranteeing that some minimum requirements are met, this approach introduces a further loop into the design process and, more important, it is unlikely to lead to a product with optimal design-point and offdesign performance; introducing some consideration of robustness actively in the design process can produce improvements in the real-world performance.

For robustness analysis to play an active role during the design process, the minimization of computational costs is paramount. In recent years, polynomial chaos has emerged as a reliable and relatively inexpensive technique (compared with Monte Carlo simulations) for obtaining high-order information for stochastic systems. In this work, a methodology for computing the probability density function for the performance of a generic modular core compression system from a three-spool gas turbine engine has been developed. Given the complexity of the system under consideration, a modification of the governing equations is not advisable; a nonintrusive formulation allows the same results to be obtained without requiring the modification of the evaluation tools used for the deterministic analysis. To improve the convergence of the method and to make any input distributions tractable, a nonintrusive adaptive-chaos approach, in which the system of orthogonal (or orthonormal) polynomials defining the chaos basis are calculated relative to the specific PDF, has been suggested, leading to improved performance relative to the use of the standard orthogonal polynomials from the Askey scheme. Nodes and weights are calculated efficiently based on the desired quadrature order. Detailed derivation is presented for a case in which the noise factor's PDF can be expressed as a polynomial of any order; alternatively, the same solution could be obtained numerically for a nonpolynomial PDF. The cost of the method, orders of magnitude less expensive than MCS, facilitates its integration into the design process, with the potential of improving the real-world performance of engine systems and subsystems.

In this work, the validity of the described approach has been demonstrated in the calculation of the variability in performance of a gas turbine's generic modular-core compression system under uncertain operating conditions. First, the variability in performance generated by a given PDF for the engine throttle (expressed through the ratio $T_{0,4}/T_{0,2}$) has been calculated. Then, the method has been expanded to account for additional uncertain parameters (air bleed and power offtake). In consideration of the rapid increase in computational time required in the presence of multidimensional uncertainties, a method for reducing the number of collocation points has been suggested. The effect of the variation in other components' performance has not been considered, but it could be included without particular difficulties, given the required performance-analysis tools. The same approach could be easily applied to any other non-deterministic problem in the presence of any type of noise factors (such as manufacturing variability or performance degradation due to wear), given that an estimation of their probability density function is available.

References

- [1] Keane, A. J., and Nair, P. B., *Computational Approaches for Aerospace Design*, Wiley, New York, 2005.
- [2] Phadke, M. S., *Quality Engineering Using Robust Design*, Prentice-Hall International Editions, Upper Saddle River, NJ, 1989.
- [3] Oberkampf, W. L., and Trucano, T. G., "Verification and Validation in Computational Fluid Dynamics," *Progress in Aerospace Sciences*, Vol. 38, 2002, pp. 209–272. doi:10.1016/S0376-0421(02)00005-2
- [4] Walters, R. W., and Huyse, L., "Uncertainty Analysis for Fluid Mechanics with Applications," NASA, CR 211449, 2002.
- [5] Putko, M. M., Newman, P. A., Taylor, A. C., and Green, L. L., "Approach for Uncertainty Propagation and Robust Design in CFD Using Sensitivity Derivatives," AIAA Paper 2001-2528, 2001.
- [6] Xiu, D., Lucor, D., Su, C.-H., and Karniadakis, G. E., "Stochastic Modeling of Flow-Structure Interaction Using Generalized Polynomial Chaos," *Journal of Fluids Engineering*, Vol. 124, No. 1, 2002, pp. 51–59. doi:10.1115/1.1436089
- [7] Wiener, N., "The Homogeneous Chaos," *American Journal of Mathematics*, Vol. 60, No. 4, 1938, pp. 897–936. doi:10.2307/2371268
- [8] Cameron, R. H., and Martin, W. T., "The Orthogonal Development of Nonlinear Functionals in Series of Fourier-Hermite Polynomials," *Annals of Mathematics*, Vol. 48, No. 2, 1947, pp. 385–392. doi:10.2307/1969178
- [9] Ghanem, R., and Spanos, P., *Stochastic Finite Elements: A Spectral Approach*, Springer-Verlag, New York, 1991.
- [10] Lucor, D., Xiu, D., and Karniadakis, G., "Spectral Representations of Uncertainty in Simulations: Algorithms and Applications," *Journal of Fluids Engineering*, Vol. 124, 2002, pp. 51–59. doi:10.1115/1.1436089
- [11] Xiu, D., and Karniadakis, G. E., "The Wiener-Askey Polynomial Chaos for Stochastic Differential Equations," *SIAM Journal on Scientific Computing*, Vol. 24, No. 2, 2002, pp. 619–644. doi:10.1137/S1064827501387826
- [12] Wan, X., and Karniadakis, G. E., "Multi-Element Generalized Polynomial Chaos for Arbitrary Probability Measures," *SIAM Journal on Scientific Computing*, Vol. 28, No. 3, 2006, pp. 901–928. doi:10.1137/050627630
- [13] Ghanem, R., "Stochastic Finite Elements for Heterogeneous Media with Multiple Random Non-Gaussian Properties," *Journal of Engineering Mechanics*, Vol. 125, 1999, pp. 26–40. doi:10.1061/(ASCE)0733-9399(1999)125:1(26)
- [14] Ghanem, R., Red-Horse, J., and Sarkar, A., "Modal Properties of a Space-Frame with Localized System Uncertainties," 8th ASCE Speciality Conference of Probabilistic Mechanics and Structural Reliability, American Society of Civil Engineers, Paper PMC2000-269, 2000.
- [15] Le Maître, O. P., Reagan, M. P., Najm, H. N., Ghanem, R. G., and Knio, O. M., "A Stochastic Projection Method for Fluid Flow: Part II, Random Process," *Journal of Computational Physics*, Vol. 181, No. 1, 2002, pp. 9–44. doi:10.1006/jcph.2002.7104
- [16] Le Maître, O. P., Knio, O. M., Debusschere, B. J., Najm, H. N., and Ghanem, R. G., "A Multigrid Solver for Two-Dimensional Stochastic Diffusion Equations," *Computer Methods in Applied Mechanics and Engineering*, Vol. 192, 2003, pp. 4723–4744. doi:10.1016/S0045-7825(03)00457-2
- [17] Xiu, D., and Karniadakis, G. E., "Modeling Uncertainty in Flow Simulations via Generalized Polynomial Chaos," *Journal of Computational Physics*, Vol. 187, No. 1, 2003, pp. 137–167. doi:10.1016/S0021-9991(03)00092-5
- [18] Walters, R. W., "Towards Stochastic Fluid Mechanics via Polynomial Chaos," 41st AIAA Aerospace Sciences Meeting and Exhibit, AIAA Paper 2003-0413, 2003.
- [19] Perez, R., and Walters, R. W., "An Implicit Compact Polynomial Chaos Formulation for the Euler Equations," 43rd AIAA Aerospace Sciences Meeting and Exhibit, Paper 2005-1406, 2005.
- [20] Mathelin, L., Hussaini, M. Y., Zang, T. A., and Bataille, F., "Uncertainty Propagation for a Turbulent, Compressible Nozzle Using Stochastic Methods," *AIAA Journal*, Vol. 42, No. 8, 2004, pp. 1669–1676. doi:10.2514/1.5674
- [21] Debusschere, B. J., Najm, H. N., Pebay, P. P., Knio, O. M., Ghanem, R. G., and Le Maître, O. P., "Numerical Challenges in the Use of Polynomial Chaos Representations for Stochastic Processes," *SIAM Journal on Scientific Computing*, Vol. 26, No. 2, 2004, pp. 698–719. doi:10.1137/S1064827503427741
- [22] Mathelin, L., and Hussaini, M. Y., "A Stochastic Collocation Algorithm for Uncertainty Analysis," NASA, CR 212153, 2003.
- [23] Loeven, A., Witteveen, J., and Bijl, R., "Probabilistic Collocation: An Efficient nonintrusive Approach for Arbitrarily Distributed Parametric Uncertainties," 45th AIAA Aerospace Sciences Meeting and Exhibit, AIAA Paper 2007-317, Reno, NV, 2007.
- [24] Hosder, S., Walters, R. W., and Balch, M., "Efficient Sampling for Nonintrusive Polynomial Chaos Applications with Multiple Uncertain Input Variables," 48th AIAA/SME/ASCE/AHS/ASC Structures, Structural Dynamics and Materials Conference, Honolulu, HI, AIAA Paper 2007-1939, 2007.

- [25] Ghisu, T., *Robust Aerodynamic Design Optimisation of Compression Systems*, Ph.D. Thesis, Univ. of Cambridge, Cambridge, England, U.K., 2009.
- [26] Jarrett, J. P., Ghisu, T., and Parks, G. T., "On the Coupling of Designer Experience and Modularity in the Aerothermal Design of Turbomachinery," *Journal of Turbomachinery*, Vol. 131, No. 3, 2009, Paper 031018.
doi:10.1115/1.2992513
- [27] Ghisu, T., Parks, G. T., Jarrett, J. P., and Clarkson, P. J., "An Integrated System for the Aerodynamic Design of Compression Systems—Part I: Development," *Journal of Turbomachinery* (to be published).
- [28] Ghisu, T., Parks, G. T., Jarrett, J. P., and Clarkson, P. J., "An Integrated System for the Aerodynamic Design of Compression Systems—Part II: Application," *Journal of Turbomachinery* (to be published).
- [29] Choen, H., Rogers, G. F. C., and Saravanamuttoo, H. I. H., *Gas Turbine Theory*, Longman Scientific & Technical, Essex, England, U.K., 1987.
- [30] Cumpsty, N. A., *Jet Propulsion*, Cambridge Univ. Press, Cambridge, England, U.K., 1997.
- [31] Lefebvre, A. H., *Gas Turbine Combustion*, Taylor & Francis, Philadelphia, 1998.
- [32] Le Maître, O. P., Reagan, M. P., Najm, H. N., Ghanem, R. G., and Knio, O. M., "A Stochastic Projection Method for Fluid Flow: Part I, Basic Formulation," *Journal of Computational Physics*, Vol. 173, No. 2, 2001, pp. 481–511.
doi:10.1006/jcph.2001.6889
- [33] Monegato, G., *Fondamenti di Calcolo Numerico*, Edizioni Clut, Torino, Italy, 1998.
- [34] Gautschi, W., "On Generating Orthogonal Polynomials," *SIAM Journal on Scientific and Statistical Computing*, Vol. 3, No. 3, 1982, pp. 289–317.
doi:10.1137/0903018
- [35] Stieltjes, T. J., "Quelques Recherches sur la Théorie des Quadratures Dites Mécaniques," *Annales Scientifique de l'École Normale Supérieure*, Vol. 1, Ser. 3, 1884, pp. 409–426; http://www.numdam.org/item?id=ASENS_1884_3_1__409_0.
- [36] Davis, P. J., and Rabinowitz, P., *Methods of Numerical Integration*, Academic Press, New York, 1984.
- [37] Nobile, F., Tempone, R., and Webster, C. G., "A Sparse Grid Stochastic Collocation Method for Partial Differential Equations with Random Input Data," *SIAM Journal on Numerical Analysis*, Vol. 46, No. 5, 2008, pp. 2309–2345.
doi:10.1137/060663660
- [38] Smolyak, S. A., "Quadrature and Interpolation Formulas for Tensor Products of Certain Classes of Functions," *Doklady Akademii Nauk SSSR*, Vol. 148, 1963, pp. 1042–1045.
- [39] Gerstner, T., and Griebner, M., "Dimension-Adaptive Tensor-Product Quadrature," *Computing*, Vol. 71, 2003, pp. 65–87.
doi:10.1007/s00607-003-0015-5
- [40] Ganapathysubramanian, B., and Zabaras, N., "Sparse Grid Collocation Schemes for Stochastic Natural Convection Problems," *Journal of Computational Physics*, Vol. 225, 2007, pp. 652–685.
doi:10.1016/j.jcp.2006.12.014

K. Willcox
Associate Editor